Edge effects in bilayer graphene nanoribbons: *Ab initio* total-energy density functional theory calculations

Matheus P. Lima,[1,*] A. Fazzio,[1,2,†] and Antônio J. R. da Silva[1,‡]
[1]*Instituto de Física, Universidade de São Paulo, CP 66318, 05315-970 São Paulo, São Paulo, Brazil*
[2]*Centro de Ciências Naturais e Humanas, Universidade Federal do ABC, Santo André, 09210-170 São Paulo, Brazil*
(Received 16 January 2009; published 2 April 2009)

We show that the ground state of zigzag bilayer graphene nanoribbons is nonmagnetic. It also possesses a finite gap, which has a nonmonotonic dependence with the width as a consequence of the competition between bulk and strongly attractive edge interactions. All results were obtained using *ab initio* total-energy density functional theory calculations with the inclusion of parametrized van der Waals interactions.

DOI: 10.1103/PhysRevB.79.153401 PACS number(s): 73.22.−f, 61.48.De, 71.15.Nc, 72.80.Rj

Since the synthesis of graphene,[1] a plethora of intriguing properties have been found in this two-dimensional zero-gap crystal due to the presence of massless fermions with a high mobility.[2,3] Besides the monolayer, stacking two layers of graphene still preserves the high mobility,[4] and some features of the electronic spectrum can be controlled, for example, by applying an external electric field.[5] Measurements of quantum Hall effect and quasiparticle band structure indicate qualitative differences between monolayers and bilayers. The occurrence of this rich physics at room temperature[6,7] has attracted a great interest in designing graphene-based nanoelectronic devices. In this scenario, it is fundamental to establish and control an energy gap (E_g).

A possibility is to introduce lateral quantum confinement via synthesis of single-layer graphene nanoribbons (GNRs) (Refs. 8 and 9) or bilayer graphene nanoribbons (B-GNRs) (Refs. 10 and 11) by plasma etching or chemical routes.[12,13] This opens a gap that raises the possibilities of using graphene in nanoelectronics, where small widths (sub-10-nm) are required for room-temperature applications.[7] However, the B-GNRs are less sensitive to external perturbations in comparison with GNRs; hence, they may be more appropriate in fabricating high-quality nanodevices.[14]

The electronic structures of the nanoribbons, including the gap, are largely affected by the geometric pattern (zigzag or armchair) at their edges. GNRs with zigzag edges, in particular, have as a distinct feature the presence of edge states that introduce a large density of states (DOS) at the Fermi energy. Theoretical works predict that this configuration is unstable, and there will be the appearance of a magnetic order that leads to the removal of this large DOS peak.[8,9,15] Magnetism in GNRs has been intensively investigated as a possible way to develop spintronic devices.[16–18] An antiferromagnetic (AF) [ferromagnetic (F)] order between the two edges leads to a semiconductor (metallic) state.[8,9,15] It is also believed that magnetism is necessary to open a gap in zigzag bilayer graphene nanoribbon (B-ZGNR).[19]

In this Brief Report we investigate the geometrical and electronic structure of B-ZGNR, and show that the ground state of these systems is *nonmagnetic and possesses a nonmonotonic finite gap*. There are two possible edge alignments for the B-ZGNR, called α and β (see Fig. 1). We found that the α alignment is energetically favorable, with an interlayer edges' attraction, whereas for the β alignment there is an interlayer edges' repulsion. These edge-related forces cause a deviation from the exact Bernal stacking, resulting in a nonmonotonic behavior of the energy gap with the width w for the α B-ZGNR, with a maximum value at $w \approx 3.5$ nm. These results differ qualitatively from single-layer graphene nanoribbons with zigzag edges (M-ZGNRs).[12,13]

All our results are based on *ab initio* total-energy density functional theory[20] (DFT) calculations. In order to correctly describe multilayer graphitic compounds, it is necessary to include van der Waals (vdW) interactions. The use of fully relaxed total-energy DFT calculations to study such systems suffers from serious limitations, since the most traditional exchange-correlation (xc) functionals in use today do not correctly describe these terms. With the local-density approximation (LDA) xc, the geometry is correctly described but the interlayer binding energy is underestimated by 50%, whereas the generalized gradient approximations' (GGAs) xc does not even correctly describe the geometrical features.[21] Thus, in order to be able to investigate the geometries and relative energies of B-ZGNRs, we include a nonlocal potential in the Kohn-Sham (KS) equations that correctly describes the vdW interactions. We modified the SIESTA code,[24] adding in the KS Hamiltonian[25] the dispersion-corrected atom-centered potential (DCACP).[26] This correction is sufficiently accurate to describe weakly bonded systems[27] with the vdW interactions included in the whole self-consistent cycle, providing accurate values for both forces (and thus

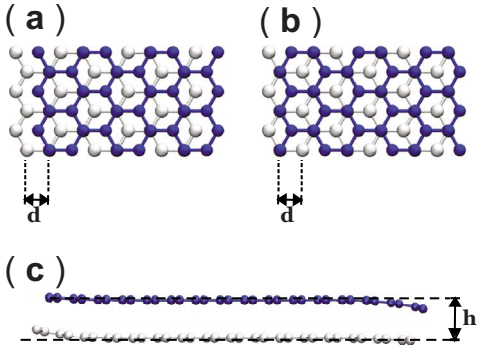

FIG. 1. (Color online) Bilayer graphene nanoribbons with (a) α and (b) β edge alignments. (c) Side view of bilayer graphene nanoribbons (α alignment). The dark (blue) and white atoms form the upper and bottom layers, respectively.

TABLE I. Interlayer binding energy (E_b) (in eV/atom) and distance h (in Å) for graphite and a graphene bilayer, which is not bound (NB) at the GGA level.

		Present	Expt.	LDA	GGA(PBE)
Graphite	E_b	0.054	0.052 ± 0.005 [a]	0.030	0.003
	h	3.350	3.356[b]	3.200	4.5
Bilayer	E_b	0.027		0.017	NB
	h	3.320		3.202	NB

[a]From Ref. 22.
[b]From Ref. 23.

geometries) and total energies. Our implementation was successfully tested (see Table I), and was employed to obtain the results here reported.[29–31]

We investigated B-ZGNR composed of two M-ZGNRs passivated with hydrogen, and with widths[32] that range from $w=0.6$ to $w=4.5$ nm. The layers are in the Bernal stacking, which means that there are two types of C atoms, those that are positioned above the center of the hexagons of the other layer, defining a B sublattice, and those right on top of the C atoms of the other layer, forming an A sublattice. An infinite graphene bilayer has no gap, and the orbitals at the Fermi level are located at the B sublattice. When we cut the layer along the zigzag edge, there are two possible alignments (Fig. 1): (a) the α alignment, where the outermost edge atoms belong to the A sublattice, and (b) the β alignment, where the outermost edge atoms belong to the B sublattice. Thus, only the interlayer edge interaction differs. Two geometrical distortions have proven to be important: (i) an edge distortion that causes a curvature in the ribbons [see Fig. 1(c)], and (ii) a lateral deviation from the perfect Bernal stacking. To quantify this deviation, we define the quantity $u \equiv d_{\text{C-C}} - d$, where d is shown in Figs. 1(a) and 1(b), and $d_{\text{C-C}}$ is the carbon-carbon bond length. The perfect Bernal stacking corresponds to $u=0$.

The geometries and band structures of fully relaxed B-ZGNRs with $w \approx 1.0$ nm for α and β alignments are presented in Fig. 2. In B-ZGNR with the β alignment, similarly as with M-ZGNRs, a non-spin-polarized calculation leads to a high DOS at the Fermi energy, and a magnetic order is required to split these localized edge states at the K symmetry point. In order to establish the possible spin-polarized configurations, we used four initial guesses for the density matrix before starting the self-consistency cycle, which are (i) AF inlayer and interlayer, (ii) F inlayer and interlayer, (iii) AF inlayer and F interlayer, and (iv) F inlayer and AF interlayer, as well as nonpolarized calculations. From all calculations, the AF inlayer and interlayer guess leads to the lower-energy state [Fig. 2(b)]. However, the energy differences are less than $k_B T$.[19]

At the α alignment [Fig. 2(a)], on the other hand, we obtain a qualitatively different situation. There is a strong attractive interaction between the edge atoms of the two layers, with a resulting geometric distortion that decreases the distance between them [Fig. 2(a)]. For all α B-ZGNRs that we have investigated, the final geometry always had an interlayer edge atoms' distance of around 3.0 Å. The final configuration is nonmagnetic and with a finite gap, contrary to previous results where the presence of a gap was intrinsically coupled to a magnetic state.[19] Note that if we do not allow the atoms at the two layers to relax, but simply optimize the interlayer distance (i.e., the layers keep their planar geometries), a magnetic configuration is still necessary to open a gap.[19] However, this configuration has higher energy.

If we take one of the monolayers that form the final relaxed α B-ZGNR and perform a calculation without letting the atoms relax, we obtain an energy increase, when compared to the lowest-energy M-ZGNR (AF inlayer[16]), which can be broken down into two components. Considering M-ZGNR with widths larger than 2 nm, if we allow the distorted monolayer to be magnetic, the energy increase is ≈ 0.1 eV/nm, which can be viewed as the elastic contribution. If we now consider a nonmagnetic configuration for this distorted monolayer, which is the situation in the α B-ZGNR, there is an extra energy increase of ≈ 0.4 eV/nm, i.e., an overall energy penalty of ≈ 0.5 eV/nm. Considering the two monolayers, the total-energy cost of deforming and demagnetizing the α B-ZGNR is ≈ 0.96 eV/nm. This energy increase is more than compensated for by the edge atoms' interaction, and the energy gain is in part associated with a large split of the localized edge states. At the β B-ZGNR [Fig. 2(b)], the unique way to diminish the DOS

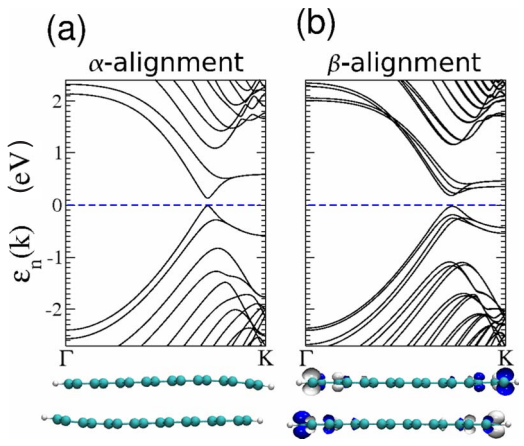

FIG. 2. (Color online) Ground state of fully relaxed B-ZGNRs generated by stacking two (7,0) M-ZGNRs. Below each band structure the geometry [large dark (small white) spheres are C (H) atoms] and local magnetization [dark (white) represents up (down) spins] are presented. (a) α alignment. This state is nonmagnetic and presents a geometric distortion near the edge. (b) β alignment. This state shows an AF inlayer and AF interlayer magnetic order.

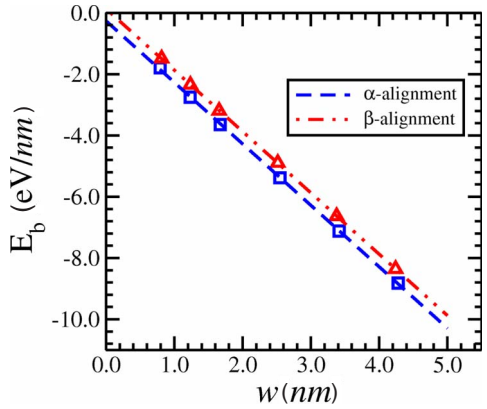

FIG. 3. (Color online) Dependence of the binding energies on the width.

associated with the localized edge states at the Fermi energy is via a magnetic ordering, and the system tends to increase the interlayer edge atoms' distance in order to allow a bigger magnetization, giving rise to a repulsive interlayer edge interaction.

Comparing the two alignments, the α B-ZGNR results are energetically favorable. This is an even more important conclusion considering that most of the calculations used the β B-ZGNR.[11,33] Figure 3 presents the dependence of the B-ZGNRs binding energies, for both edge alignments, as a function of w (calculated relative to two isolated lowest-energy M-ZGNRs). The interaction between the layers can be separated into two components: (i) edge interactions, which do not depend on the width, and (ii) and bulk interactions, which increase linearly with w. The binding energies (per unit length) can be well adjusted with

$$E_b(w) = a + bw. \tag{1}$$

Since there are two edges, $a/2$ is the interlayer edge interaction energy per unit length, and b is the interlayer bulk interaction energy per unit area. At the α alignment, $a=-0.26$ eV/nm and $b=-2.0$ eV/nm^2, indicating that the edges' interaction is attractive ($a<0$). For the β alignment, $a=+0.13$ eV/nm and $b=-2.0$ eV/nm^2, indicating that there is a repulsive edges' interaction ($a>0$), showing that its stability results solely from the bulk. The parameter b, as expected, does not depend on the edge alignment, and it is very close to our calculated bulk interlayer interaction in a graphene bilayer (0.027 eV/atom$=-1.99$ eV/nm^2).

For the α B-ZGNR, there is a competition between the forces deriving from the bulk, which do prefer the Bernal pattern of stacking, and the forces deriving from the edges, which tend to maintain the interlayer edge carbon atoms' distance close to 3 Å. The system then minimizes the overall energy penalty by simultaneously optimizing both the deviation u from the exact Bernal stacking and the elastic energy associated with the ribbon's curvature. Thus, for narrower B-ZGNR the system prefers to have a larger value of u and a smaller overall curvature. On the other hand for wider B-ZGNR the deviation u tends to decrease to minimize the bulk energy penalty, since now it is possible to have a softer curvature that is somewhat localized at the edges when compared to the total width of the ribbon [see Fig. 1(c)]. As a result, the dependence of the lateral deviation u on the width w is well adjusted by $u(w)=0.80e^{-0.35w}$ (with u in angstroms, and w in nanometers). Moreover, as a result, the carbon-carbon bond lengths do not significantly differ from their values in the M-ZGNRs. For this situation, the average interlayer distance h is close to its value in the graphene bilayer (see Table I).

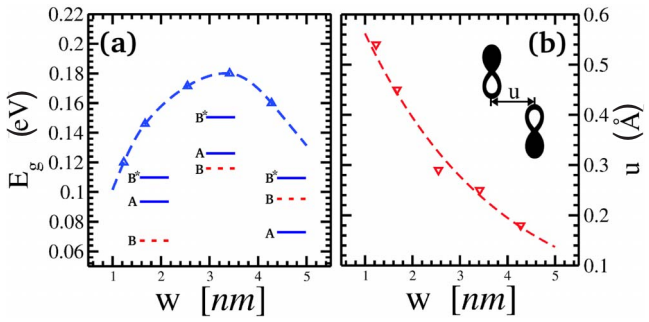

FIG. 4. (Color online) Dependences of the (a) energy gap (inset illustrates the change of character of the VBM) and (b) the lateral deviation u on the width w (inset indicates how u affects the interlayer A-sublattice p-orbital interaction).

Without the geometrical deformation caused by the interlayer edge interactions, a monotonic decrease in the energy gap is expected due to the quantum confinement ($\propto 1/w$).[9,19] However, for small ribbons, we find that the character of the valence-band maximum (VBM) is located at the A sublattice, as opposed to larger ribbons where it is located in the B sublattice [see Fig. 4(a)], similarly as with the Fermi-level orbitals in the infinite graphene bilayer. Moreover, since the interaction between the C atoms in the A sublattice increases when u decreases [see Fig. 4(b)], the gap initially increases with w. However, for $w \gtrsim 3.5$ nm, due to the quantum-confinement decrease, there is a crossover between the two highest occupied bands, and the character of the VBM is at the B sublattice. Thus, this leads to a nonmonotonic behavior of the energy gap with w [Fig. 4(a)].

For the β B-ZGNR, there is a repulsive interaction between the edges, in such a way that the interlayer edge carbon atoms' distance is close to 3.7 Å. There occurs a small negative lateral deviation ($u<0$) that can be neglected when $w>1.6$ nm. Note that for the α B-ZGNR, due to the attractive edges' interaction, $u>0$. We also found that, despite the presence of a magnetic order, the energy gap disappears when $w>3$ nm.

Summarizing, we unequivocally show that for B-ZGNR the edge alignment α is the lowest-energy configuration. This is a result of the strong attractive interaction between the edges, which is manifested in an observed chemical bonding between the interlayer edge carbon atoms, and which significantly influences the geometry and electronic structure of bilayer nanoribbons with sub-10-nm widths. As a consequence, the ground state is nonmagnetic and possesses a finite gap, which presents a nonmonotonic dependence on the width.

We acknowledge helpful discussions with M. D. Coutinho-Neto regarding the DCACP and financial support from FAPESP and CNPq.

*mplima@if.usp.br
†fazzio@if.usp.br
‡ajrsilva@if.usp.br

[1] K. S. Novoselov, A. K. Geim, S. V. Morozov, D. Jiang, Y. Zhang, S. V. Dubonos, I. V. Grigorieva, and A. A. Firsov, Science **306**, 666 (2004).
[2] K. S. Novoselov, Z. Jiang, Y. Zhang, S. V. Morozov, H. L. Stormer, U. Zeitler, J. C. Maan, G. S. Boebinger, P. Kim, and A. K. Geim, Nature (London) **438**, 197 (2005); Y. B. Zhang, Y. W. Tan, H. L. Stormer, and P. Kim, *ibid.* **438**, 201 (2005).
[3] A. H. Castro Neto, F. Guinea, N. M. R. Peres, K. S. Novoselov, and A. K. Geim, Rev. Mod. Phys. **81**, 109 (2009).
[4] K. S. Novoselov, E. McCann, S. V. Morozov, V. I. Fal'ko, M. I. Katsnelson, U. Zeitler, D. Jiang, F. Schedin, and A. K. Geim, Nat. Phys. **2**, 177 (2006).
[5] T. Ohta, A. Bostwick, T. Seyller, K. Horn, and E. Rotenberg, Science **313**, 951 (2006); E. V. Castro, K. S. Novoselov, S. V. Morozov, N. M. R. Peres, J. M. B. Lopes dos Santos, J. Nilsson, F. Guinea, A. K. Geim, and A. H. Castro Neto, Phys. Rev. Lett. **99**, 216802 (2007); J. B. Oostinga, H. B. Heersche, X. L. Liu, A. F. Morpurgo, and L. M. K. Vandersypen, Nature Mater. **7**, 151 (2008).
[6] K. S. Novoselov, Z. Jiang, Y. Zhang, S. V. Morozov, H. L. Stormer, U. Zeitler, J. C. Maan, G. S. Boebinger, P. Kim, and A. K. Geim, Science **315**, 1379 (2007); N. Tombros, C. Jozsa, M. Popinciuc, H. T. Jonkman, and B. J. van Wees, Nature (London) **448**, 571 (2007).
[7] X. R. Wang, Y. J. Ouyang, X. L. Li, H. L. Wang, J. Guo, and H. J. Dai, Phys. Rev. Lett. **100**, 206803 (2008).
[8] Y. W. Son, M. L. Cohen, and S. G. Louie, Phys. Rev. Lett. **97**, 216803 (2006).
[9] L. Yang, C. H. Park, Y. W. Son, M. L. Cohen, and S. G. Louie, Phys. Rev. Lett. **99**, 186801 (2007).
[10] K.-T. Lam and G. Liang, Appl. Phys. Lett. **92**, 223106 (2008).
[11] E. V. Castro, N. M. R. Peres, and J. M. B. Lopes dos Santos, J. Optoelectron. Adv. Mater. **10**, 1716 (2008).
[12] M. Y. Han, B. Ozyilmaz, Y. B. Zhang, and P. Kim, Phys. Rev. Lett. **98**, 206805 (2007).
[13] X. L. Li, X. R. Wang, L. Zhang, S. W. Lee, and H. J. Dai, Science **319**, 1229 (2008).
[14] Y. M. Lin and P. Avouris, Nano Lett. **8**, 2119 (2008).
[15] L. Pisani, J. A. Chan, B. Montanari, and N. M. Harrison, Phys. Rev. B **75**, 064418 (2007).
[16] T. B. Martins, R. H. Miwa, A. J. R. da Silva, and A. Fazzio, Phys. Rev. Lett. **98**, 196803 (2007).
[17] Y. W. Son, M. L. Cohen, and S. G. Louie, Nature (London) **444**, 347 (2006).
[18] E. J. Kan, Z. Y. Li, J. L. Yang, and J. G. Hou, J. Am. Chem. Soc. **130**, 4224 (2008).
[19] B. Sahu, H. Min, A. H. MacDonald, and S. K. Banerjee, Phys. Rev. B **78**, 045404 (2008).
[20] P. Hohenberg and W. Kohn, Phys. Rev. **136**, B864 (1964); W. Kohn and L. J. Sham, *ibid.* **140**, A1133 (1965).
[21] M. Hasegawa, K. Nishidate, and H. Iyetomi, Phys. Rev. B **76**, 115424 (2007), and references therein.
[22] R. Zacharia, H. Ulbricht, and T. Hertel, Phys. Rev. B **69**, 155406 (2004).
[23] A. Bosak, M. Krisch, M. Mohr, J. Maultzsch, and C. Thomsen, Phys. Rev. B **75**, 153408 (2007).
[24] E. Artacho, D. Sanchez-Portal, P. Ordejon, A. Garcia, and J. M. Soler, Phys. Status Solidi B **215**, 809 (1999).
[25] The added matrix elements are $H_{\mu\nu}^{\mathrm{DCACP}} = \Sigma_j \Sigma_{m=-l}^{l} \langle \varphi_\mu p_j^{lm} \rangle \sigma_j^1 \langle p_j^{lm} \varphi_\nu \rangle$, where $\{\varphi_\mu\}$ are the localized bases. We use only $l=3$, and centered at each atom j there is a normalized projector $p_j^{lm}(\mathbf{r}) \propto Y_{lm}(\hat{\mathbf{r}}) r^l \exp(\frac{-r^2}{2\sigma_2^2})$, where Y_{lm} are spherical harmonics. The parameters (σ_1, σ_2) are from Ref. 28.
[26] O. A. von Lilienfeld, I. Tavernelli, U. Rothlisberger, and D. Sebastiani, Phys. Rev. Lett. **93**, 153004 (2004).
[27] E. Tapavicza, I. C. Lin, O. A. von Lilienfeld, I. Tavernelli, M. D. Coutinho-Neto, and U. Rothlisberger, J. Chem. Theory Comput. **3**, 1673 (2007); O. A. von Lilienfeld, I. Tavernelli, U. Rothlisberger, and D. Sebastiani, Phys. Rev. B **71**, 195119 (2005).
[28] I. Chun Lin, M. D. Coutinho-Neto, C. Felsenheimer, O. A. von Lilienfeld, I. Tavernelli, and U. Rothlisberger, Phys. Rev. B **75**, 205131 (2007).
[29] We use a generalized gradient approximation (Ref. 30), norm-conserving pseudopotentials (Ref. 31), a mesh cutoff of 400 Ry for the grid integration, a $1 \times 1 \times 50$ mesh for the first Brillouin-zone sampling, a force criterion of 10 meV/Å, and a supercell approximation with a lateral separation between the images of 20 Å.
[30] J. P. Perdew, K. Burke, and M. Ernzerhof, Phys. Rev. Lett. **77**, 3865 (1996).
[31] N. Troullier and J. L. Martins, Phys. Rev. B **43**, 1993 (1991).
[32] We have defined the width as the lateral distance between the outermost C edge atoms of the bilayer.
[33] E. V. Castro, N. M. R. Peres, J. M. B. Lopes dos Santos, A. H. Castro Neto, and F. Guinea, Phys. Rev. Lett. **100**, 026802 (2008); J. Rhim and K. Moon, J. Phys.: Condens. Matter **20**, 365202 (2008).